Virology 420 (2011) 89–97

Contents lists available at SciVerse ScienceDirect

Virology

journal homepage: www.elsevier.com/locate/yviro

Replication of *Lettuce chlorosis virus* (LCV), a crinivirus in the family *Closteroviridae*, is accompanied by the production of LCV RNA 1-derived novel RNAs

Chawin Mongkolsiriwattana, Angel Y.S. Chen, James C.K. Ng *

Department of Plant Pathology and Microbiology, University of California, Riverside, CA 92521, USA

ARTICLE INFO

Article history:
Received 8 July 2011
Returned to author for revision 31 July 2011
Accepted 25 August 2011
Available online 26 September 2011

Keywords:
Lettuce infectious yellows virus
Defective RNA
5′-terminal RNA
Subgenomic RNA
Cloned infectious cDNAs

ABSTRACT

Cloned infectious complementary DNAs of the bipartite genomic RNAs of *Lettuce chlorosis virus* (LCV) were constructed. Inoculation of tobacco protoplasts with the *in vitro* produced RNAs 1 and 2 transcripts, or with RNA 1 transcript alone, resulted in viral replication accompanied by the production of novel LCV RNA 1-derived RNAs. They included the abundantly accumulating LM-LCVR1-1 (~0.38 kb) and LM-LCVR1-2 (~0.3 kb), and the lowly accumulating HM-LCVR1-1 (~8.0 kb) and HM-LCVR1-2 (~6.6 kb), all of which reacted with riboprobes specific to the 5′ end of RNA 1 in Northern blot analysis. LM-LCVR1-1 and HM-LCVR1-2 accumulated as positive-stranded RNAs that lacked complementary negative strands, while HM-LCVR1-1 and LM-LCVR1-2 accumulated in both polarities. Additional Northern blot, reverse transcription-polymerase chain reaction, cloning, and sequence analyses revealed LM-LCVR1-2 to be an authentic RNA 1-derived defective (D)RNA, suggesting that its synthesis and maintenance are supported *in trans* by an RNA 1 encoded replication machinery.

Published by Elsevier Inc.

Introduction

The genus *Crinivirus* in the family *Closteroviridae* contains whitefly transmitted viruses that are emerging and economically important. Criniviruses have single-stranded positive-sense bipartite RNA genomes, and share two common genomic features with other members of the family: 1) a replication module consisting of a papain-like leader proteinase (P-PRO), a methyltransferase (MTR), and a helicase (HEL) encoded in open reading frame 1a (ORF 1a), and an RNA-dependent RNA polymerase (RdRp) encoded in ORF 1b; and 2) a hallmark closterovirus gene array containing ORFs encoding a small hydrophobic protein, a heat shock protein homolog (HSP70h), a protein of 50–60 kDa, the major coat protein (CP) and the minor coat protein (CPm) (Agranovsky, 1996; Dolja et al., 2006; Karasev, 2000; Martelli et al., 2002).

Lettuce chlorosis virus (LCV) is a newly described crinivirus whose genome sequence we have recently determined (Salem et al., 2009). The LCV genome consists of at least 13 ORFs, with ORFs encoding P23, HSP70h, P60, CP, CPm and P27 being expressed via a nested set of 3′-coterminal subgenomic (sg)RNAs (Salem et al., 2009). The 3′ non-coding regions (NCRs) of the LCV genomic RNAs share a relatively high level of sequence identity, a feature that is common among all criniviruses except for *Lettuce infectious yellows virus* (LIYV) (Aguilar et al., 2003; Hartono et al., 2003; Klaassen et al., 1995; Kreuze et al., 2002; Lozano et al., 2009; Okuda et al., 2010; Salem et al., 2009; Tzanetakis et al., 2006; Wintermantel et al., 2009; Wintermantel et al., 2005), and has been hypothesized to contribute to a similar temporal accumulation of both viral genomic RNAs (Salem et al., 2009). In Northern blot analyses of the total RNA extracts of LCV infected plants, a positive-sense specific riboprobe corresponding to the 5′-proximal end of RNA 1 reacted with a low molecular weight (MW) (~0.3–0.4 kb) RNA, while that corresponding to the 5′-proximal end of RNA 2 reacted with several low MW (~0.4–1.5 kb) RNAs (Salem et al., 2009). These RNAs resemble the positive-stranded 5′-coterminal sgRNAs, referred to as 'low MW tristeza (LMT) RNAs', produced by *Citrus tristeza virus* (CTV; family *Closteroviridae*) (Che et al., 2001; Gowda et al., 2009; Mawassi et al., 1995b). CTV also produces positive-stranded 5'-coterminal sgRNAs, referred to as 'large MW tristeza (LaMT) RNAs', that are ~10 kb in size (Che et al., 2001). However, negative-stranded LMT and LaMT RNAs have not been observed. In the case of LCV, because it is not known if the low MW RNAs are coterminal in sequence at their 5′ ends, they have been referred to as LCV 5′-terminal RNAs. Whether or not these LCV 5′-terminal RNAs are lacking in negative strands and whether the equivalents of LaMT RNAs are produced during LCV infection are unknown.

So far, LIYV is the only crinivirus to have cloned genomic (cDNA) components that are biologically active when delivered to protoplasts and plants (Klaassen et al., 1996; Ng and Falk, 2006; Wang et al., 2009a). Unlike RNAs 1 and 2 of LCV, those of LIYV exhibit an asynchronous accumulation pattern where the accumulation of RNA 2

* Corresponding author at: Department of Plant Pathology and Microbiology, 900 University Ave., University of California, Riverside, CA 92521, USA. Fax: +1 951 827 4294.
E-mail address: jamesng@ucr.edu (J.C.K. Ng).

0042-6822/$ – see front matter. Published by Elsevier Inc.
doi:10.1016/j.virol.2011.08.017

lags behind that of RNA 1 in the early stages of infection (Yeh et al., 2000). This phenomenon has been postulated to be partly due to the dissimilarity in sequence and/or structure in the 3' NCRs of both genomic RNAs (Buck, 1996; Dreher, 1999; Yeh et al., 2000).

The differences in temporal accumulation of LIYV and LCV genomic RNAs, as well as the production of the LCV RNA 1 low MW RNAs (Salem et al., 2009; Yeh et al., 2000) prompted us to construct the cloned cDNAs corresponding to the full-length genomic RNAs of LCV for use in studies to understand LCV RNA replication. Inoculation of tobacco protoplasts with the LCV RNA 1 and 2 transcripts demonstrated their biological activity. More importantly, viral replication was accompanied by the production of unique LCV RNA 1-derived RNAs that were either previously not seen, or were observed but not investigated. They included a low MW 5′-terminal RNA that resembled the LMT RNA of CTV, two high MW RNAs (with one resembling the LaMT RNA of CTV), and an authentic RNA 1 defective (D)RNA. The generation of an RNA 1 DRNA is remarkable for it has never been reported for LIYV or any other criniviruses. Furthermore, protoplast inoculation with only the LCV RNA 1 transcript showed that these novel RNAs were produced and accumulated over time. These data demonstrated the complexity of the LCV RNA 1 replication machinery, and provided new evidence that the replication mechanism of LCV differed from that of LIYV.

Results

Construction of cloned full-length cDNAs of LCV RNAs 1 and 2

The complete genome sequence information of LCV (Salem et al., 2009) facilitated to generate the cloned cDNAs corresponding to LCV RNAs 1 and 2 to develop a reverse genetics system. We used LCV vRNA as the source of genetic material for reverse transcription and long template PCR, which generated cDNAs with adenylated 3′ ends. This allowed the cDNA corresponding to full-length LCV RNA 1 to be directly cloned into a vector with 3′ thymidine overhangs (pGEM-T Easy) (Materials and methods; Supplementary Fig. 1A). A similar approach was used to clone the cDNA of LCV RNA 2 but the desired full-length product could not be obtained after several attempts. Consequently, we employed an alternate cloning strategy, where two overlapping cDNA fragments (nucleotides 1–4096 and 3964–8556) corresponding to LCV RNA 2 were generated and subsequently assembled (Materials and methods; Supplementary Figs. 2A and B). Sequence analysis of these cloned cDNAs found nucleotides and deduced amino acids that differed from the published LCV sequences (Salem et al., 2009). In total, there were 12 genomic locations where polymorphisms were observed (Figs. 1A and B).

To verify that the cloned cDNAs contained all the genetic information necessary to sustain biological activity, further modifications were made. First, both constructs were designed to contain a modified bacteriophage T3 promoter where two of the three terminal guanine residues at the 3′ end were removed (Supplementary Figs. 1B and 2C). This ensured that the first nucleotide (guanine) incorporated into the *in vitro* synthesized transcripts corresponded to the first nucleotide in the LCV genomic RNAs. Second, the cloned cDNA constructs were each modified to contain a NgoMIV restriction site directly downstream of the 3′-terminus of the LCV sequences. This design enabled the first nucleotide in the restriction recognition sequence to correspond to the last nucleotide of the LCV genomic RNAs in both cDNA clones. Thus, digestion with this enzyme would linearize both plasmids at a position immediately after the last nucleotide of the LCV sequence (Supplementary Figs. 1B and 2C). Following the above modifications, the final cloned cDNAs, named pCM1 and pCM2 (Supplementary Figs. 1B and 2C), were expected to produce transcripts bearing authentic LCV RNAs 1 and 2 5′- and 3′-termini upon *in vitro* synthesis (Supplementary Figs. 1C and 2D).

LCV coat protein synthesis and virion formation

We hypothesized that the *in vitro* transcripts synthesized from pCM1 and pCM2 contained all the genomic information required for biological activity in inoculated plant cells. To test this hypothesis, we assessed their ability to encode the major coat protein (CP) and determined whether or not virion formation could ensue following protoplast inoculation. Total soluble protein extracts and virions were prepared using pCM1 and pCM2 transcript-inoculated tobacco protoplasts harvested at 96 hours post-inoculation (hpi). Immunoblot analysis of SDS-PAGE-separated proteins from the total protein extract and virion preparation was performed using a LCV virion-specific polyclonal IgG. The approx. 28.4 kDa CP was observed in both the total protein extract and virion preparation samples (Fig. 1C, lanes 2 and 3). The virion preparation was also analyzed by transmission electron microscopy (TEM), which revealed the presence of crinivirus-like particles approx. 600–800 nm in length (Fig. 1D).

LCV replication in tobacco protoplasts inoculated with pCM1 and pCM2 transcripts

We next assessed the time course accumulation of LCV RNAs in protoplasts inoculated with the pCM1 and pCM2 *in vitro* synthesized transcripts. Total RNA was extracted from cells at 0, 12, 24, 48, 72, and 96 hpi and analyzed in Northern blots using DIG-labeled single stranded riboprobes II and VIII complementary to the 3'-proximal regions of the positive- and negative-sense LCV RNAs 1 and 2, respectively (Fig. 2A). Both positive- and negative-sense LCV genomic RNA 1s were visible as early as 12 hpi (Figs. 2B and C, lane 12; insets B1 and C1). Accumulation of both RNAs increased rapidly (approx. 9 fold for positive-sense and 8 fold for negative-sense) from 12 to 24 hpi, and continued to increase gradually until reaching the last time point at 96 hpi (Figs. 2B and C, lanes 12 to 96). The subgenomic RNA (sgRNA) of P8 and/or P23 (sg1) was visible at 24 hpi and accumulated rapidly to a maximum at 48 hpi (Fig. 2B).

Positive- and negative-sense LCV genomic RNA 2s were observed at 12 hpi (Figs. 2D and E, lane 12; insets D1, E1 and E2). The signal at 0 hpi was most likely from the transcript inoculum of pCM2. The accumulation of positive- and negative-sense RNA 2s increased rapidly by approximately 9 fold from 12 to 24 hpi and approximately 20 fold from 24 to 48 hpi (Figs. 2D and E, lanes 12, 24, and 48). The increase in accumulation of both RNA species then continued gradually to the last time point at 96 hpi (Figs. 2D and E, lanes 12 to 96). All the predicted RNA 2-derived sgRNAs (sg2-6) were visible as early as 48 hpi (Fig. 2D, lanes 48 to 96). Their accumulation increased slightly from 48 to 72 hpi, where the maximum accumulation was reached.

Synthesis and accumulation of novel viral RNAs

Previously, Northern blot analyses using riboprobes complementary to the 5′-proximal ends of positive-sense RNAs 1 and 2 detected several low MW viral RNAs in the total RNA extracts of LCV-infected *Chenopodium murale* plants (Salem et al., 2009). Their hybridization properties suggested that these viral RNAs were potential 5′-coterminal sgRNAs (Che et al., 2001; Gowda et al., 2001; Gowda et al., 2009; Mawassi et al., 1995b; Salem et al., 2009). Here, we focused on RNA 1 and its derivative(s) by first determining if a prominent ~0.3–0.4 kb viral RNA previously observed in infected plant samples (Salem et al., 2009) was also produced in vRNA- and transcript-inoculated protoplasts, and if it was generated in both polarities or was lacking in negative strand.

We isolated total RNA from transcript-, vRNA-, and mock (water)-inoculated protoplasts at 96 hpi and analyzed them by Northern blotting using the RNA 1 positive-sense specific probe I (Fig. 2A). The analysis identified genomic RNA 1 and an ~0.38 kb RNA, designated LM-LCVR1-1, in the total RNA extracts of transcript- and vRNA-

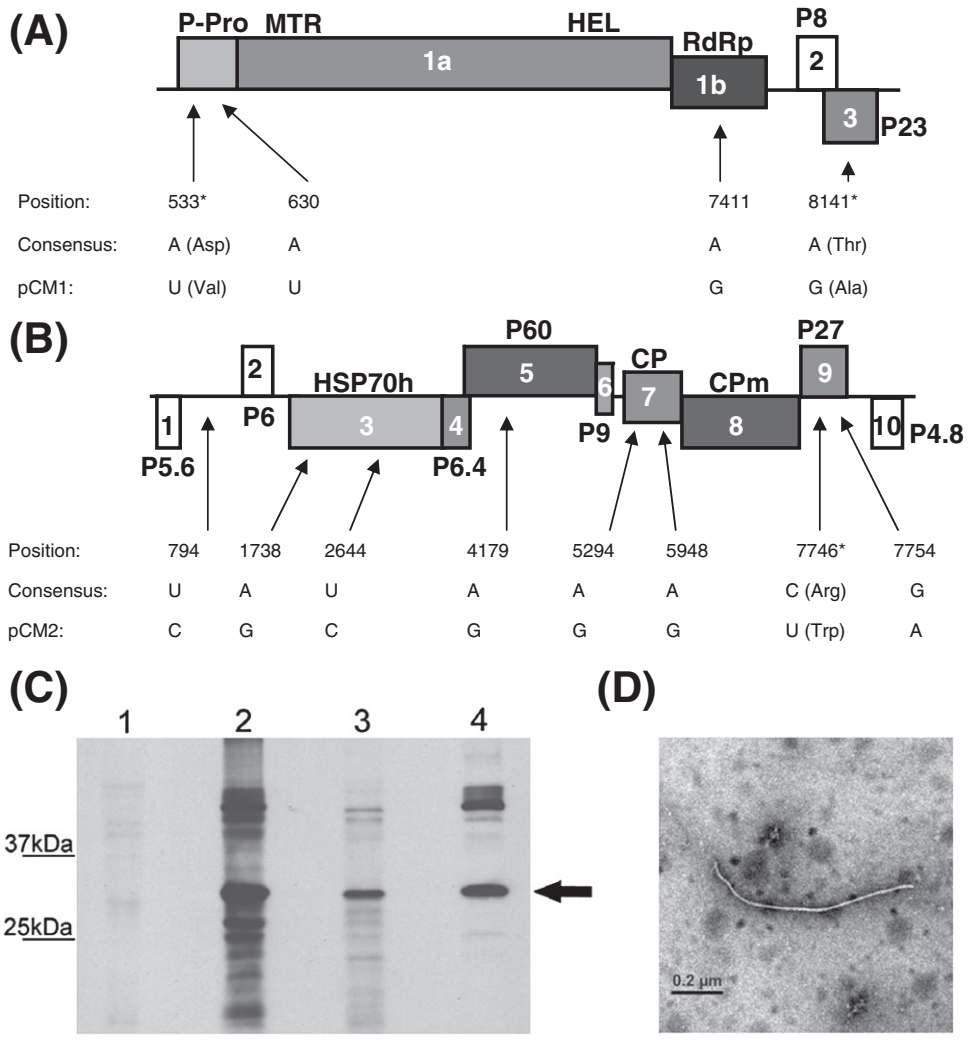

Fig. 1. Organization of: (A) LCV RNA 1 showing the differences between the consensus and pCM1 (cloned cDNA of RNA 1) sequences; and (B) LCV RNA 2 showing the differences between the consensus and pCM2 (cloned cDNA of RNA 2) sequences. Numbers in the boxes within the genome maps represent open reading frames that encode proteins or protein-domains: P-Pro, papain-like protease; MTR, methyltransferase; HEL, RNA helicase; RdRp, RNA-dependent RNA polymerase; HSP70h, a heat shock protein 70 homolog; CP, major coat protein; CPm, minor coat protein; and proteins that are named according to their relative molecular masses (numbers preceded by 'P'). Numbers and arrows below the genome maps indicate the nucleotide positions where changes (A, U, C, or G) have been observed. Nucleotide positions at which non-synonymous changes have occurred are marked by an *, with the deduced amino acid changes indicated in parentheses. (C) Immunoblot analysis of LCV virions. Virion preparation and total protein extract were separated on a 12% SDS-polyacrylamide gel, transferred onto nitrocellulose membrane, and analyzed using a polyclonal IgG produced against LCV virions. Lane 1, total soluble proteins from water (mock)-inoculated protoplasts; lane 2, total soluble proteins from pCM1 and pCM2 *in vitro* transcript-inoculated protoplasts; lane 3, virion preparation from pCM1 and pCM2 *in vitro* transcript-inoculated protoplasts; and lane 4, LCV virions purified from infected *Chenopodium murale* plants. The position of the LCV CP (28.4 kDa) is indicated by an arrow. Additional (25 kDa and 37 kDa) size markers are included as references. (D) Transmission electron microscopy analysis of the LCV virion preparation obtained from pCM1 and pCM2 *in vitro* transcript-inoculated protoplasts. A 0.2 micron scale bar is provided for size reference.

inoculated protoplasts (Fig. 3A, lanes 1 and 2) but not in that of mock (water)-inoculated protoplasts (Fig. 3A, lane 3). LM-LCVR1-1 was observed only with probe I (Fig. 3A) but not with probe II (complementary to the 3′-proximal region of RNA 1) (Figs. 2B and C), suggesting that this was not a conventional 3′-coterminal sgRNA. The positive-sense specific probe I also hybridized to multiple RNA species with sizes ranging from ~0.4 to ~1.5 kb (indicated as ♦ in Fig. 3A, lanes 1, 2 and 4). The positive-sense specific probe I further identified another distinct low MW (~0.3 kb) RNA, LM-LCVR1-2, and specific but low levels of two high MW RNAs, HM-LCVR1-1 (~8.0 kb) and HM-LCVR1-2 (~6.6 kb), from the protoplast and plant samples (Fig. 3A, lanes 1, 2 and 4).

We next used the positive- or negative-sense specific probe I to analyze the time course accumulation of LM-LCVR1-1, LM-LCVR1-2, HM-LCVR1-1, and HM-LCVR1-2. Positive-sense LM-LCVR1-1 was visible at 24 hpi and accumulated at amounts higher than genomic RNA 1 (Fig. 3B). LM-LCVR1-1 accumulated approx. 11 fold from 24 to 48 hpi, reaching a maximum at 72 hpi, and was maintained at that level up to the final sampling time of 96 hpi (Fig. 3B, lanes 24 to 96). Detectable amounts of negative strand LM-LCVR1-1 were not apparent throughout the sampling period (Fig. 3C). Positive strand HM-LCVR1-2 was visible at 48 hpi [and at 24 hpi with a prolonged exposure of the X-ray film (not shown)]; however it accumulated less drastically relative to genomic RNA 1 and LM-LCVR1-1, showing only a slight increase from 24 to 72 hpi, and was maintained at that level up to the final sampling time of 96 hpi (Fig. 3B, lanes 48 to 96). The accumulation of negative stranded HM-LCVR1-2 was not apparent throughout the sampling period (Fig. 3C, lanes 48 to 96). In contrast, LM-LCVR1-2 and HM-LCVR1-1 were hybridized by both the positive-and negative-sense specific probe I (Figs. 3B and C). Positive and negative stranded LM-LCVR1-2 were observed at 48 hpi and accumulated appreciably to a maximum at 96 hpi (Figs. 3B and C), while positive and negative stranded HM-LCVR1-1 were also observed at 48 hpi but accumulated marginally from 48 to 96 hpi compared to genomic RNA 1 and LM-LCVR1-2 (Figs. 3B and C). Accumulation of the multiple low MW RNAs seen in Fig. 3A (indicated

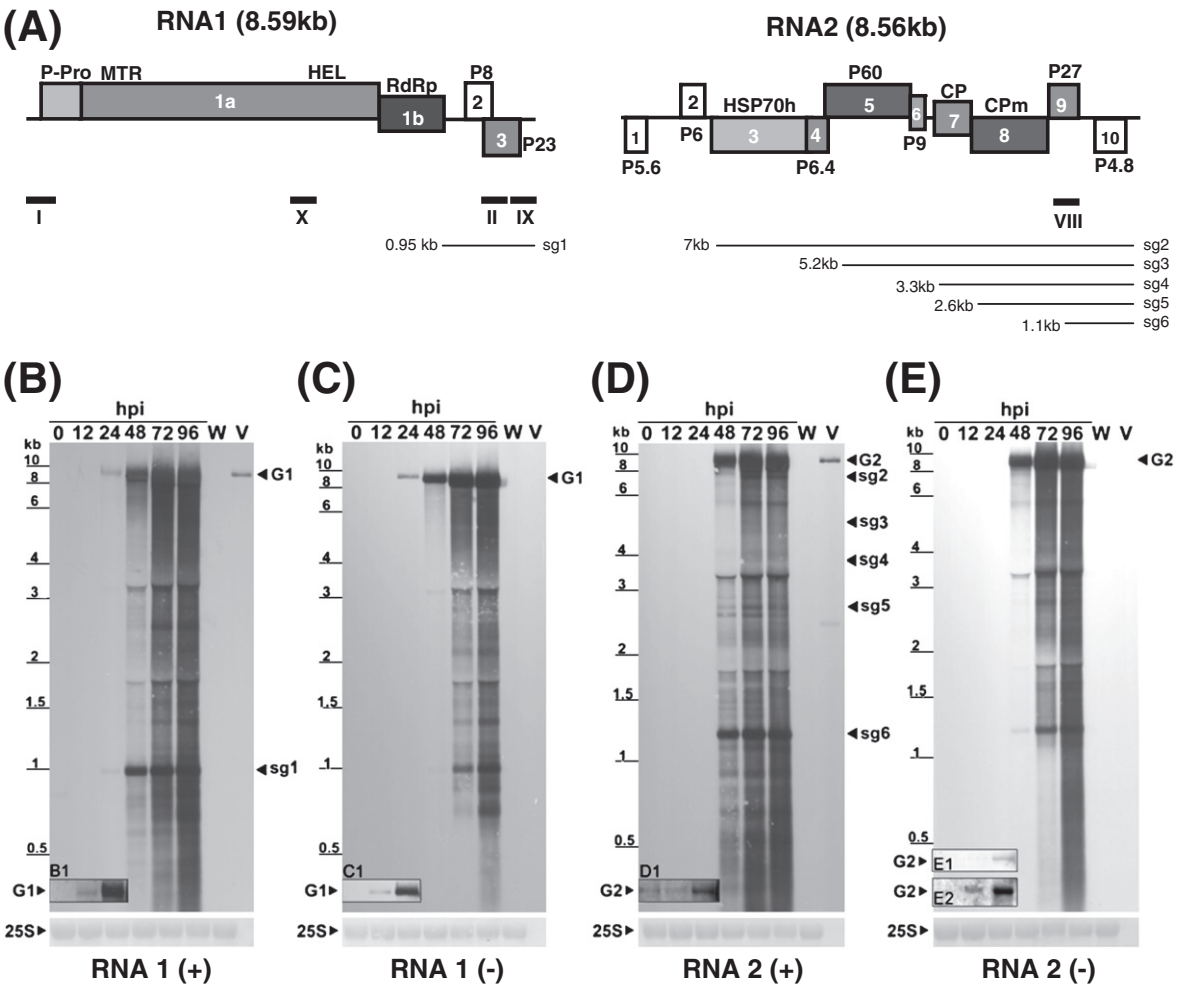

Fig. 2. Accumulation of *Lettuce chlorosis virus* (LCV) RNAs in tobacco protoplast. (A) Genome organization of LCV. Black bars below the genome map (I, II, VIII, IX and X) represent the riboprobes complementary to the corresponding locations in the LCV genomic RNAs. Fine lines beneath the black bars represent the predicted 3' co-terminal subgenomic (sg)RNAs: P8 and/or P23 (sg1), P6 and/or HSP70h (sg2), P6.4 and/or P60 (sg3), P9 and/or CP (sg4), CPm (sg5), and P27 (sg6), with sizes (kb) as indicated. (B–E) Viral RNA accumulation in tobacco protoplasts inoculated with the *in vitro* transcripts of pCM1 and pCM2. Total RNA (2 μg each) extracted from the inoculated protoplasts harvested at 0, 12, 24, 48, 72, and 96 hours post-inoculation (hpi) (lanes 0 to 96, respectively), total RNA (2 μg) from water (mock)-inoculated protoplasts harvested at 96 hpi (lane W), and LCV virion RNA (10 ng) (lane V) were analyzed using DIG-labeled positive- (B) or negative-sense (C) RNA 1 specific probe II, and positive- (D) or negative-sense (E) RNA 2 specific probe VIII. The polarity (+ or −) of viral RNAs being detected is indicated under each blot. Hybridization signals of positive- and negative-sense genomic RNAs 1 (G1) and 2 (G2), and sgRNAs 1, 2, 3, 4, 5, and 6 are indicated. Insets B1, C1, D1 and E1 show the extended exposures of the hybridization signals for the genomic RNAs (G1 or G2) in lanes 0, 12, and 24. Inset E2 shows the hybridization signals for genomic RNA 2 (G2) in lanes 0, 12, and 24 of a subsequent blot when a 2.5 fold higher amount (5 μg) of total RNA from each sample harvested at 0, 12, and 24 hpi, respectively, were analyzed. Sizes of RNAs were estimated based on methylene blue-stained RNA standards shown on the left of each blot. The methylene blue-stained 25S rRNA of each sample was included to demonstrate the equal loading of total RNA samples.

as ♦ in Figs. 3A and B) was observed when tested using positive-sense specific probe I, but were indistinct when negative-sense specific probe I was used (Fig. 3C).

Because we now have biologically active cDNA clones of the LCV genomic RNAs, it was possible to determine whether infection by RNA 1 alone would result in the production of LM-LCVR1-1, LM-LCVR1-2, HM-LCVR1-1, and HM-LCVR1-2. Using the positive- or negative-sense specific probe I in Northern blot analyses of the total RNA extracts from protoplasts inoculated with the pCM1 transcript, our results showed that all of these RNAs were produced and/or accumulated with the same kinetics as they would in cells inoculated with pCM1 and pCM2 transcripts (Figs. 3D and E). Thus, these results suggest that the production of the RNA 1-derived novel RNAs is independent of RNA 2.

Identification of an LCV RNA 1-derived defective RNA

We next performed Northern analyses on the pCM1 and pCM2 transcript-inoculated samples using the positive- or negative-sense specific probe IX, complementary to nucleotides 8331 to 8573 at the extreme 3′ terminus of LCV RNA 1 (Fig. 2A) and observed a specific RNA that corresponded to the size expected of LM-LCVR1-2 (~0.3 kb) (Figs. 4A and B). The positive strand was detected from 48 to 96 hpi, similar to the accumulation kinetics of positive strand LM-LCVR1-2. We next conducted a Northern analysis using the positive- or negative-sense specific probe X, complementary to nucleotides 3881 to 4157 in the middle region of RNA 1 (Fig. 2A) to further characterize the ~0.3 kb RNA. Neither the positive- nor negative-sense specific probe X hybridized to an RNA species of that size, although they did hybridize to the ~8.0 kb RNA (HM-LCVR1-1), while positive-sense specific probe X also hybridized to the 6.6 kb RNA (HM-LCVR1-2) as anticipated (Figs. 4C and D). These data suggested that the ~0.3 kb RNA and LM-LCVR1-2 were likely one and the same RNA species and contained DRNA features i.e. the presence of 5′ and 3′ termini of RNA 1 but absence of an internal region of the RNA. In an attempt to determine the identity of the ~0.3 kb LM-LCVR1-2, we subjected the total RNA of LCV-infected *C. murale* plants and that of pCM1 and pCM2 transcript-inoculated protoplasts harvested at 96 hpi to RT-PCR using oligonucleotide primers LCV-50 and LCV-55, complementary to the extreme 5′ and 3′ termini, respectively, of

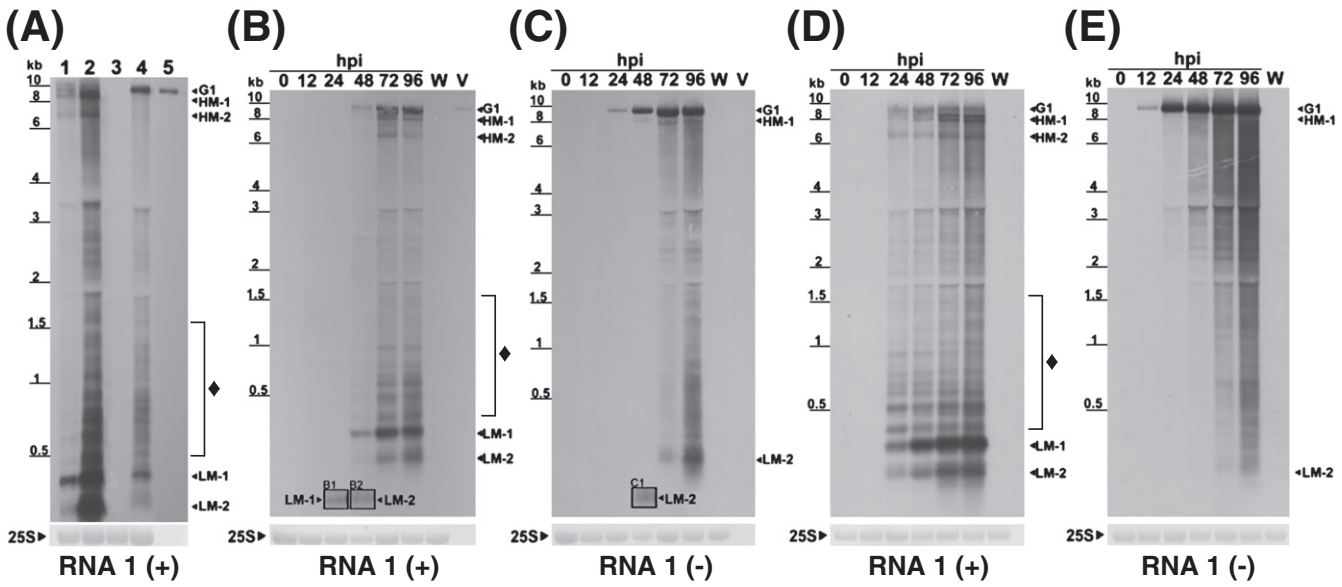

Fig. 3. Northern analysis of LCV RNA 1-derived novel RNAs. (A) Northern blot using RNA 1 (+)-specific probe I (complementary to nt positions 1–482). Samples were total RNA of tobacco protoplasts inoculated with: pCM1 and pCM2 transcripts (lane 1), LCV virion RNA (lane 2), and water (mock inoculation) (lane 3). Total RNA from LCV-infected *C. murale* plants (lane 4) and LCV virion RNA (lane 5) were included for comparison. (B) Total RNA of: pCM1 and pCM2 transcript- (lanes 0 to 96 hpi) and water (mock)-inoculated protoplasts (lane W; harvested at 96 hpi), and LCV virion RNA (V) were analyzed using RNA 1 (+)-specific probe I. (C) Northern blot analysis of the same samples in (B) using the RNA 1 (−)-specific probe I. (D) Total RNA of: pCM1 transcript- (lanes 0 to 96 hpi) and water (mock)-inoculated protoplasts (lane W; harvested at 96 hpi) were analyzed using RNA 1 (+)-specific probe I. (E) Northern blot analysis of the same samples in (D) using the RNA 1 (−)-specific probe I. The polarity (+ or -) of viral RNAs being detected is indicated under each blot. Hybridization signals of positive- and negative-sense genomic RNA 1 (G1), and the RNA 1-derived low MW and high MW RNAs: LM-LCVR1-1 (LM-1), LM-LCVR1-2 (LM-2), HM-LCVR1-1 (HM-1), and HM-LCVR1-2 (HM-2) are indicated. Extended exposures of the signals for LM-1 (inset B1) at 24 hpi, and LM-2 (insets B2 and C1) at 48 hpi, are shown at the bottom of the corresponding lanes. Hybridization signals from less distinct, unidentified RNA species are indicated by ♦. RNA size estimates and methylene blue-stained 25S rRNAs loading controls were as for Fig. 2.

RNA 1. A discrete ~0.4 kb product was generated from each sample (Fig. 5A, lanes 1 and 2) and cloned into the pGEM-T Easy plasmid. Nine to eleven recombinant plasmids containing the cDNA inserts generated from each of the above samples were randomly selected for sequencing. The cDNA inserts ranged in size from 0.3 kb to 0.4 kb and exhibited very similar nucleotide sequence arrangements with DRNA features: the presence of 5′ terminal nucleotides from position 1 to between positions 190 and 304, corresponding to the 5′ NCR and part of ORF 1a (beginning at position 73) encoding the first 39 to 77 amino acids of the P-Pro, followed immediately by 3' terminal nucleotides from between positions 8391 and 8562 to position 8591 (the last nucleotide), corresponding to the 3′ NCR of RNA 1.

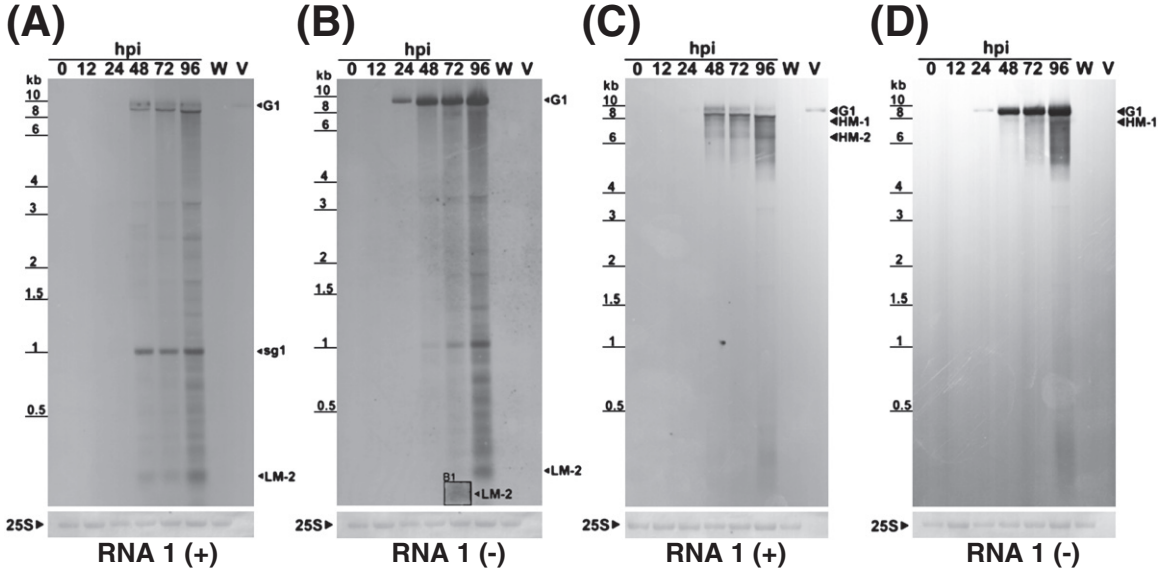

Fig. 4. Northern blot characterization of an LCV RNA 1 defective RNA. Total RNA extracted from the pCM1 and pCM2 transcript-inoculated protoplasts harvested at 0, 12, 24, 48, 72, and 96 hours post-inoculation (hpi) (lanes 0 to 96, respectively), total RNA from water (mock)-inoculated protoplasts harvested at 96 hpi (lane W), and virion RNA (lane V) were analyzed using RNA 1 (+)- (A) or RNA 1 (−)- (B) specific probe IX (nt position 8331–8573), and RNA 1 (+)- (C) or RNA 1 (−)- (D) specific probe X (nt position 3881–4157). The polarity (+ or −) of viral RNAs being detected is indicated under each blot. Hybridization signals of positive- and negative-sense genomic RNA 1 (G1), and the RNA 1-derived low MW and high MW RNAs: LM-LCVR1-2 (LM-2), HM-LCVR1-1 (HM-1), and HM-LCVR1-2 (HM-2) are indicated. The extended exposure of the hybridization signal for LM-2 (inset B1) at 72 hpi is shown at the bottom of that lane. RNA size estimates and methylene blue-stained 25S rRNAs loading controls were as for Fig. 2.

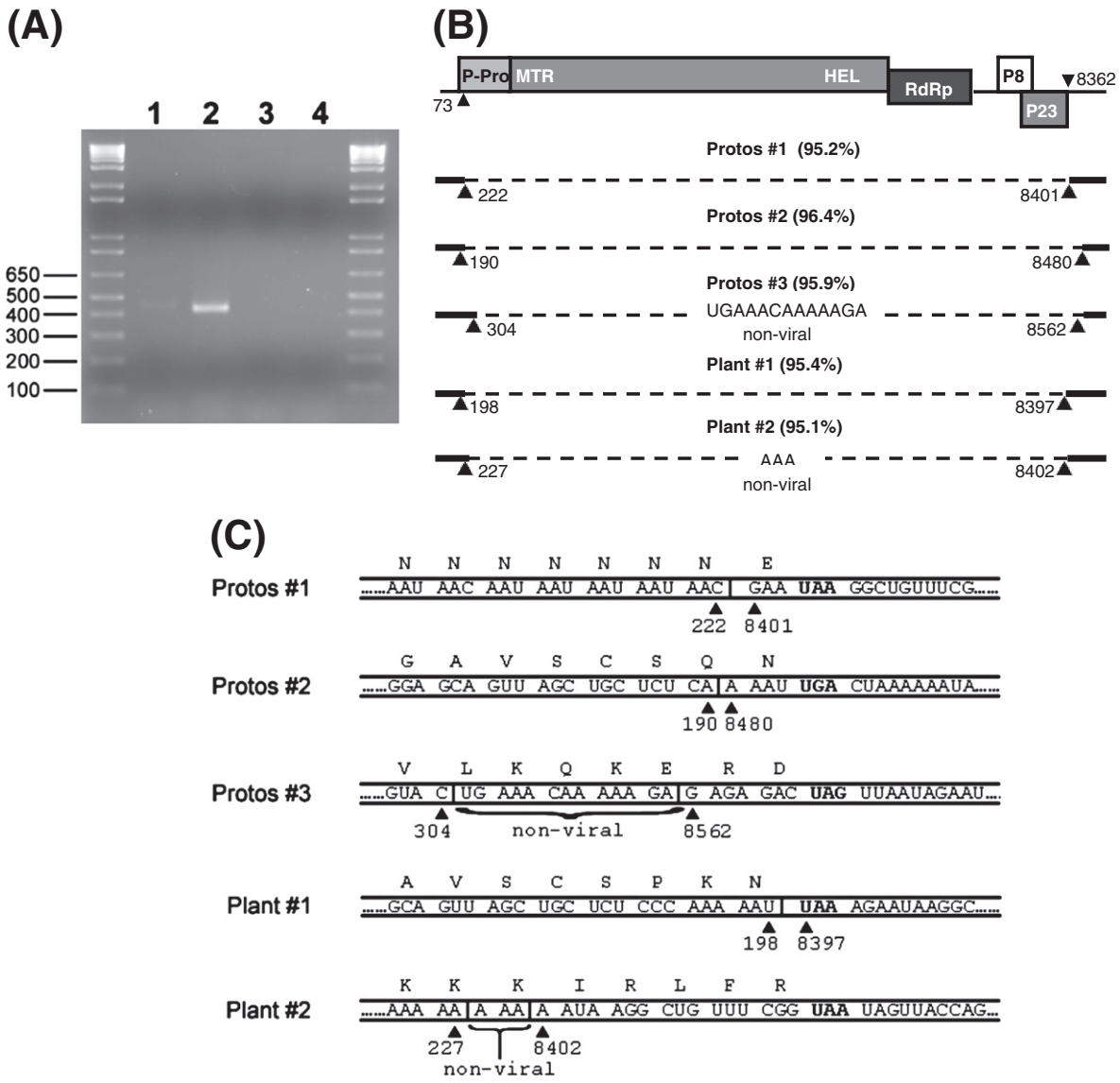

Fig. 5. Nucleotide sequence analysis of LCV RNA 1 defective (D)RNAs. (A) Ethidium bromide-stained 2% agarose gel for products amplified from the total RNA of LCV-infected plants (lane 1) and that of pCM1 and pCM2 transcript-inoculated protoplasts (lane 2) by reverse transcription and polymerase chain reaction (RT-PCR) using oligonucleotide primers specific to the extreme 5′ and 3′ termini of RNA 1. The same pair of primers and reaction conditions were used for the amplification of pCM1 transcript (lane 3) and the pCM1 plasmid (lane 4). Sizes in base pairs for DNA standards are indicated. (B) Nucleotide sequence arrangements of representative DRNAs isolated from LCV-infected protoplasts (Protos #1, #2, and #3), and LCV-infected plants (Plant #1 and #2). The LCV RNA 1 map is shown at the top. Numbers, 73 and 8362, on the map indicate the nucleotide position of the start codon of open reading frame (ORF) 1a, and the stop codon of ORF 3, respectively. Beneath the map, solid lines represent the nucleotide sequences of DRNAs; dashed lines represent regions of RNA 1 not present in the DRNAs. The numbers preceding the triangles underneath each DRNA indicate the nucleotide positions at the junctions where the loss of RNA 1 nucleotides had occurred. The percentage of RNA 1 missing from each DRNA is indicated in parenthesis. (C) Nucleotide sequences spanning the junction (represented by a vertical line or vertical lines) formed by the union of the LCV RNA 1 5′ and 3′ terminal sequences in each of the DRNAs described in (B). The nucleotide sequences are shown in triplets to represent codons within the putative ORF. Stop codons are indicated in bold; deduced amino acids are shown on top of each codon triplet. Numbers underneath the triangles represent the nucleotide positions on LCV RNA 1 where union of the 5′ and 3′ terminal sequences occurs. Dots represent the rest of the nucleotides in the DRNAs. Non-viral sequences occurring at the junctions of DRNAs in (B) and (C) are indicated.

93–96% of RNA 1 nucleotides were absent between these two nucleotide junctions. Two of the cDNA inserts contained additional (non-viral) nucleotides in between the two nucleotide junctions. Their nucleotide sequence arrangements and those of three other representative DRNAs identified from protoplasts or plants are shown in Fig. 5B. Interestingly, although the terminal regions of RNA 1 that made up these DRNAs were either non-coding sequences or contained only part of an ORF, the resulting DRNAs that formed were found to all contain a predicted small ORF of 123 to 252 nucleotides with the stop codon located in the 3′ terminal sequences (Fig. 5C). To ensure that any DRNAs identified by this strategy were not artifacts caused by the false priming of the oligonucleotide primers, we also conducted RT-PCR using full-length LCV RNA 1 transcripts as a control. No RT-PCR products were observed from the full-length LCV RNA 1 transcripts (Fig. 5A, lane 3), indicating that under similar conditions used for the RT-PCR mediated cDNA synthesis of the DRNAs, neither artifacts nor the full-length cDNA of RNA 1 were generated. As an additional control, the LCV RNA 1 transcripts were used for RT-PCR with two sets of oligonucleotide primers, LCV-50 and LCV-25, and LCV-29 and LCV-55 (see Materials and methods), which would amplify products corresponding to nucleotide position 1 to 482 and 8076 to 8591 on RNA 1, respectively. RT-PCR products of 482 and 515 nucleotides, the expected sizes, were obtained (not shown), indicating that the LCV RNA 1 transcripts were amenable to RT-PCR amplification.

We also subjected the total RNA from pCM1 transcript-inoculated protoplasts to RT-PCR using the same oligonucleotide primers and

reaction conditions as above and obtained cloned RT-PCR amplified cDNA products that all contained distinctive DRNA features and a *de novo* produced ORF similar to the ones described above (not shown).

Discussion

We have obtained the cloned full-length cDNAs corresponding to the genomic RNAs of LCV. This is only the second crinivirus for which cloned cDNAs of the viral genomic RNAs are available. While sequence identity between the 3′ NCRs of the genomic RNAs is high within most individual criniviruses, there is generally very little sequence conservation in these regions among the different criniviruses. Thus, RT-PCR synthesis of full-length cDNAs corresponding to the LCV genomic RNAs was possible only with the use of LCV-specific oligonucleotide primers, and only after the genome sequence of the virus became available (Salem et al., 2009). Sequence analysis of pCM1 and pCM2 revealed 12 nucleotides and three deduced amino acids that differed from those of the consensus sequences (Fig. 1). However, it is clear that these changes did not abolish the biological activity of the pCM1- and pCM2-derived transcripts.

Protoplasts inoculated with these transcripts produced a viral RNA accumulation profile resembling that of protoplasts inoculated with WT LCV vRNA (Salem et al., 2009). First, they supported the accumulation of negative-sense LCV genomic RNAs 1 and 2, as well as the accumulation of all predicted RNAs 1- and 2-derived sgRNAs. The accumulation of sgRNAs 3 and 4 was not readily apparent (Fig. 2), although this was consistent with the results of our previous study using LCV-infected plant tissues and LCV vRNA-inoculated tobacco protoplasts (Salem et al., 2009). Thus, it seems likely that sgRNAs 3 and 4 are either synthesized at low amounts or are turned-over quickly in LCV infected cells relative to the other predicted sgRNAs. Second, viral genomic RNAs exhibited a temporally similar accumulation pattern early in the infection. This was supported by results shown in Fig. 2 wherein both positive- and negative-sense LCV RNAs 1 and 2 were detected within approximately 12 hpi. Third, protoplasts inoculated with pCM1- and pCM2-derived transcripts produced crinivirus-like particles and CPs that were readily detected by TEM and immunoblots, respectively (Figs. 1C and D).

A comparison of the viral RNA accumulation profiles in pCM1 and pCM2 transcript-, pCM1 transcript-alone, and vRNA-inoculated protoplasts, as well as of LCV-infected plants revealed that LCV replication is accompanied by the production of RNA 1-derived low MW and high MW RNAs (Figs. 3 and 4). LM-LCVR1-1 and HM-LCVR1-2, in having only positive stranded forms and accumulating at different levels, clearly possess features that are similar to those of 5′-coterminal sgRNAs/ 5′-terminal RNAs such as CTV LMT and LaMT RNAs, respectively (Che et al., 2001). Synthesis of the CTV LMT RNAs involve the participation of controller elements (CEs) located in the 5′ region within ORF 1a of the CTV genome (Che et al., 2001; Gowda et al., 2003; Mawassi et al., 1995a). The CTV CEs are hypothesized to fold into unique stem loops, whose assumed role is to disrupt the progression of the replicase complex, although mutagenesis studies suggested that the secondary structures and primary sequences of these CEs are both required for optimal sgRNA synthesis (Gowda et al., 2001, 2003). Intriguingly, although a high MW (~7 kb) RNA 1-derived 5′ sg-like RNA has been previously observed in the dsRNA preparation of LIYV-infected plants (Rubio et al., 2000), abundantly accumulating low MW 5′-terminal RNAs like LM-LCVR1-1 have never been reported for LIYV or any other criniviruses. In the case of HM-LCVR1-1, both positive and negative strands were observed. However, neither the mechanism by which they are synthesized nor those for the production of the 5'-terminal RNAs (LM-LCVR1-1 and HM-LCVR1-2) is understood. If CEs regulating the synthesis of the 5′-terminal RNAs exist, then based on our data, they would likely be found within the coding regions of ORFs 1a and 1b in RNA 1.

An important result from this study is the identification of an authentic LCV RNA 1-derived DRNA, LM-LCVR1-2, since DRNAs that are derived entirely from RNA 1 have never before been reported for LIYV or any other criniviruses (Rubio et al., 2000). A previous study reported that DRNAs of the crinivirus *Potato yellow vein virus* (PYVV) were found to contain nucleotide sequences originating from parts of RNA 1. However, these DRNAs also contained nucleotide sequences that originated from other regions of the PYVV genome (Eliasco et al., 2006). RT-PCR results from our study indicated that the ~0.3–0.4 kb DRNAs generated from the total RNA of both LCV-infected plants and protoplasts were similar in size to that of the ~0.3 kb LM-LCVR1-2 observed in Northern blot analysis, (Fig. 5A, lanes 1 and 2, and Fig. 3A lanes 1, 2 and 4). Several of the RNA 1 DRNAs contained extra nucleotide repeats at the junction sites (Fig. 5B), and were consistent with those observed for the DRNAs of CTV (Mawassi et al., 1995a, 1995b) as well as for several RNA 2 DRNAs of LIYV (Rubio et al., 2000). Also consistent with the results obtained from studies of CTV DRNAs was the discovery of a putative *de novo* generated small ORF in the LCV RNA 1 DRNA (Yang et al., 1997). The significance of this putative ORF is unclear; however, as demonstrated by Mawassi et al. (2000), the putative ORF in the CTV DRNAs was required for their replication and accumulation.

By inoculating protoplasts only with the pCM1 (LCV RNA 1) transcript and still observing the generation of 5′-terminal RNAs and DRNAs, it is clear that their synthesis are coupled to the activities of RNA 1. RNA 1's involvement in the maintenance of the DRNA, LM-LCVR1-2, is especially noteworthy for it has important implications on the replication mechanism of LCV and other criniviruses. In order for it to propagate, the DRNA has to contain all the necessary information as well as sequence and/or structural signals required for replication. However, without any complete sequences (of ORF 1a and 1b) encoding for the replication associated proteins, this function must most likely be supplied *in trans* by the helper WT RNA 1. In striking contrast, LIYV RNA 1 does not appear to support the *trans* replication of any RNA 1 DRNAs, whether they are naturally occurring or artificially constructed (Wang et al., 2009b). The lack of naturally occurring LIYV RNA 1-derived DRNAs, among other lines of evidence such as the observation that RNAs 1 and 2 do not accumulate in a synchronous manner, and the abundance of RNA 2-derived DRNAs have led to the proposal of a *cis* preferential model of replication for LIYV RNA 1 (Rubio et al., 2000; Wang et al., 2009b; Yeh et al., 2000). For LCV, we now know that its RNA 1 supports the replication of a DRNA *in trans*. However, if *cis* preferential replication exists for LCV RNA 1, based on our data, it is unlikely that it is regulated by a mechanism similar to that of LIYV. Thus, although LIYV RNA 1 *in cis* replication is the initial step in the asynchronous replication of the LIYV genomic RNAs (Wang et al., 2009b), this mechanism may not be universally applicable to or identical in all criniviruses.

Materials and methods

Construction of full-length LCV RNAs 1 and 2 cDNA clones

All oligonucleotide primers used for the construction of full-length LCV RNAs 1 and 2 cDNA clones are indicated in Supplementary Table 1. The first strand cDNA of LCV RNA1 was generated using purified LCV virion RNAs (vRNA), the oligonucleotide primer LCV-55, and ThermoScript™ Reverse Transcriptase (Invitrogen, Carlsbad, CA) according to the manufacturer's instructions. Second-strand cDNA synthesis and PCR amplification was performed using the Expand Long Template PCR system (system 1; Roche) with the oligonucleotide primers LCV-55 and LCV-52 according to the manufacturer's instructions. The product was separated by agarose gel electrophoresis and purified using the QIAquick Gel Extraction Kit (Qiagen, Valencia, CA). The resulting product was ligated into the pGEM-T

Easy vector (Promega Corp., Madison, WI), to yield the full-length LCV RNA 1 cDNA clone, p101 (Supplementary Fig. 1A).

The bacteriophage T3 promoter was engineered immediately upstream of the 5′-terminus of the LCV sequence in p101 by PCR using p101 as template, and oligonucleotide primers LCV-89-CN and LCV-90-CN. The amplified product was gel-purified, adenylated and cloned into the pGEM-T Easy vector (Promega) to yield the intermediate clone, p102 (not shown). A DNA fragment of p101 was removed by digesting with NcoI and AflII restriction enzymes (New England Biolab) and subsequently replacing it with the similarly digested T3-containing fragment from p102 (not shown), producing the intermediate clone p103 (not shown).

A NgoMIV restriction site was engineered immediately downstream of the LCV RNA 1 3'-terminus in p103 by PCR using p101 as the template and oligonucleotide primers LCV-91-CN and LCV-92-CN. The amplified product was gel-purified, adenylated and cloned into the pGEM-T Easy vector to yield the intermediate clone p104 (not shown). A DNA fragment of p104 was removed by digesting with HpaI and NdeI and subcloned into similarly digested p103, producing pCM1 (Supplementary Fig. 1B).

The development of the full-length LCV RNA 2 cDNA clone began with the synthesis of two RT-PCR fragments (1 + 2) using vRNA as the template (Supplementary Fig. 2A). Fragment 1, corresponding to LCV RNA 2 nucleotides 1–4096, was generated using the oligonucleotide primers LCV-88-JN and LCV-56-JN. The product was cloned into the pGEM-T Easy vector, resulting in p201.1 (Supplementary Fig. 2A).

The bacteriophage T3 promoter was engineered immediately upstream of the 5'-terminus of the LCV RNA 2 sequence in p201.1 using a PCR-mediated approach essentially similar to the one used for constructing pCM1, except that p201.1 was used as the template for PCR involving the oligonucleotide primers LCV-101-CM and LCV-124-CM. The amplified product was cloned into the pGEM-T Easy vector and digested with KasI and NcoI restriction enzymes. The KasI and NcoI digested fragment was replaced with a similarly digested fragment from p201.1 to yield p202 (Supplementary Fig. 2B).

Fragment 2, corresponding to LCV RNA 2 nucleotide 3964–8556, was generated using the oligonucleotide primers LCV-57-JN and LCV-87-JN. The amplified product was cloned into the pGEM-T Easy vector, resulting in p201.2 (Supplementary Fig. 2A). The product was subsequently digested with AatII and NcoI restriction enzymes and cloned into similarly digested p202, resulting in p203 (Supplementary Fig. 2B).

Finally, a NgoMIV restriction site was introduced immediately downstream of the LCV RNA 2 3'-terminus in p201.2, similar to the construction of pCM1, except that it involved the oligonucleotide primers LCV-125-CM and LCV-104-CM. The amplified product was gel-purified, adenylated and cloned into pGEM-T Easy vector. The clone was digested with AatII and ApaI restriction enzymes and cloned into similarly digested p203, producing pCM2 (Supplementary Fig. 2C).

Standard molecular procedures were performed according to Sambrook and Russell (Sambrook and Russell, 2001). All PCR amplifications were performed using Turbo *Pfu* polymerase (Stratagene, La Jolla, CA) unless otherwise stated. All cDNA clones were transformed into *Escherichia coli* DH5α competent cells and grown in Luria-Bertani broth containing ampicillin (100 μg/ml; Sigma-Aldrich, St. Louis, MO). All cloned products derived from PCR-amplification were sequenced in both directions.

Protoplast inoculation and downstream analyses: Northern blot, Immunoblot, virion purification and TEM, cDNA cloning, and sequencing

In vitro transcription of pCM1 and pCM2 followed the procedures as previously described (Ng et al., 2004), except that the plasmids were linearized with NgoMIV restriction enzyme. *Nicotiana tabacum* var. Xanthi (tobacco) protoplast preparation and inoculation with LCV vRNAs, the *in vitro* synthesized transcripts of wild type (WT) pCM1 and pCM2 or of WT pCM1 alone were essentially similar to that previously described (Ng et al., 2004; Salem et al., 2009) except 2 μg of each of the *in vitro* synthesized transcripts were used for inoculation.

Total RNA extraction of inoculated protoplasts and infected plants were performed as previously described (Ng et al., 2004; Salem et al., 2009). Approximately 2 μg (unless otherwise stated) of total RNA from each sample were analyzed by Northern Blot using DIG-labeled riboprobes I (nts 1–482) and II (nts 7813–8179), specific to RNA 1, and VIII (nts 7428–7817) specific to RNA 2 as previously described (Fig. 2) (Salem et al., 2009). Two additional DIG-labeled riboprobes, IX (nts 8331–8573) and X (nts 3881–4157), specific to RNA 1 were generated in this study following the previously described methods (Fig. 2) (Salem et al., 2009). Digoxigenin chemiluminescent signals of RNA-probe hybrids captured on X-ray films were estimated by densitometry using the Scion Image software (Scion Corp.).

Purification of virions from LCV infected *C. murale* plants and from protoplasts inoculated with the pCM1 and pCM2 *in vitro* synthesized transcripts was performed according to the procedures described in Ng et al. (2004). Total soluble proteins were extracted as previously described in Klaassen et al. (1996). Immunoblot analyses of total soluble protein and purified virions were performed according to Ng and Falk (2006), except that a LCV virion-specific polyclonal IgG was used at a 1:300 fold dilution, and cross absorbed with 2.5%(w/v) *N. benthamiana* leaf extracts prepared in 10%(w/v) non-fat dried milk with 1x PBST (10 mM Na_2HPO_4, 2 mM KH_2PO_4, 2.7 mM KCl, 137 mM NaCl, 0.3% Tween 20, pH 7.4). The purified virions were subjected to transmission electron microscopy analysis as previously described (Tian et al., 1999).

To determine the nucleotide sequences of the DRNAs that were produced during LCV replication, the total RNA extracts of LCV infected *C. murale* plants and tobacco protoplasts (inoculated with the *in vitro* produced transcripts of pCM1 and pCM2, or of pCM1 alone and harvested at 96 hpi) were subjected to reverse transcription (RT) to generate the first strand cDNA. The RT reaction was performed using the oligonucleotide primer LCV-55 and M-MLV Reverse Transcriptase (Promega Corp., Madison, WI) according to the manufacturer's instructions. Second-strand cDNA synthesis and PCR were performed using the oligonucleotide primers LCV-50 [5'-GAAATCAAACTTTCCTTCG-3′, corresponding to LCV RNA 1 position 1 to 19] and LCV-55. The above oligonucleotide primers were also used for the RT-PCR and PCR amplification of control templates: pCM1 *in vitro* transcripts and the pCM1 plasmid, respectively. To verify that they were good templates for RT-PCR, the pCM1 *in vitro* produced transcripts were subjected to RT-PCR using two sets of oligonucleotide primers: LCV-25 [5′-GGCATCCTGTTAAATCTGCA-3′, complementary to LCV RNA 1 position 482–463] and LCV-50, and LCV-55 and LCV-29 [5′-TACAGGAAGACCTGTTACTGTTACA-3′, corresponding to LCV RNA 1 position 8076–8100]. All PCR amplifications were performed using *Taq* DNA polymerase. The cloning of the RT-PCR products into the pGEM-T Easy vector and the subsequent sequencing steps were as described above.

Supplementary materials related to this article can be found online at doi:10.1016/j.virol.2011.08.017

Acknowledgments

This work was supported by start-up funds provided by the College of Natural and Agricultural Sciences of the University of California, Riverside to J.C.K.N.

We thank Carlo Natividad and Tongyan Tian for technical assistance, and Bryce Falk for helpful discussion.

References

Agranovsky, A.A., 1996. Principles of molecular organization, expression, and evolution of closteroviruses: over the barriers. Adv. Virus Res. 47, 119–158.

Aguilar, J.M., Franco, M., Marco, C.F., Berdiales, B., Rodriguez-Cerezo, E., Truniger, V., Aranda, M.A., 2003. Further variability within the genus *Crinivirus*, as revealed by determination of the complete RNA genome sequence of *Cucurbit yellow stunting disorder virus*. J. Gen. Virol. 84 (9), 2555–2564.

Buck, K.W., 1996. Comparison of the replication of positive-stranded RNA viruses of plants and animals. Adv. Virus Res. 47, 159–251.

Che, X., Piestun, D., Mawassi, M., Yang, G., Satyanarayana, T., Gowda, S., Dawson, W.O., Bar-Joseph, M., 2001. 5'-coterminal subgenomic RNAs in *Citrus tristeza virus*-infected cells. Virology 283 (2), 374–381.

Dolja, V.V., Kreuze, J.F., Valkonen, J.P., 2006. Comparative and functional genomics of closteroviruses. Virus Res. 117 (1), 38–51.

Dreher, T.W., 1999. Functions of the 3'-untranslated regions of positive strand RNA viral genomes. Annu. Rev. Phytopathol. 37, 151–174.

Eliasco, E., Livieratos, I.C., Muller, G., Guzman, M., Salazar, L.F., Coutts, R.H., 2006. Sequences of defective RNAs associated with *Potato yellow vein virus*. Arch. Virol. 151 (1), 201–204.

Gowda, S., Satyanarayana, T., Ayllon, M.A., Albiach-Marti, M.R., Mawassi, M., Rabindran, S., Garnsey, S.M., Dawson, W.O., 2001. Characterization of the *cis*-acting elements controlling subgenomic mRNAs of *Citrus tristeza virus*: production of positive- and negative-stranded 3'-terminal and positive-stranded 5'-terminal RNAs. Virology 286 (1), 134–151.

Gowda, S., Ayllon, M.A., Satyanarayana, T., Bar-Joseph, M., Dawson, W.O., 2003. Transcription strategy in a *Closterovirus*: a novel 5'-proximal controller element of *Citrus tristeza virus* produces 5'- and 3'-terminal subgenomic RNAs and differs from 3' open reading frame controller elements. J. Virol. 77 (1), 340–352.

Gowda, S., Tatineni, S., Folimonova, S.Y., Hilf, M.E., Dawson, W.O., 2009. Accumulation of a 5' proximal subgenomic RNA of *Citrus tristeza virus* is correlated with encapsidation by the minor coat protein. Virology 389 (1–2), 122–131.

Hartono, S., Natsuaki, T., Genda, Y., Okuda, S., 2003. Nucleotide sequence and genome organization of *Cucumber yellows virus*, a member of the genus *Crinivirus*. J. Gen. Virol. 84 (4), 1007–1012.

Karasev, A.V., 2000. Genetic diversity and evolution of closteroviruses. Annu. Rev. Phytopathol. 38, 293–324.

Klaassen, V.A., Boeshore, M.L., Koonin, E.V., Tian, T., Falk, B.W., 1995. Genome structure and phylogenetic analysis of *Lettuce infectious yellows virus*, a whitefly-transmitted, bipartite *Closterovirus*. Virology 208 (1), 99–110.

Klaassen, V.A., Mayhew, D., Fisher, D., Falk, B.W., 1996. *In vitro* transcripts from cloned cDNAs of the *Lettuce infectious yellows closterovirus* bipartite genomic RNAs are competent for replication in *Nicotiana benthamiana* protoplasts. Virology 222 (1), 169–175.

Kreuze, J.F., Savenkov, E.I., Valkonen, J.P., 2002. Complete genome sequence and analyses of the subgenomic RNAs of *Sweet potato chlorotic stunt virus* reveal several new features for the genus *Crinivirus*. J. Virol. 76 (18), 9260–9270.

Lozano, G., Grande-Perez, A., Navas-Castillo, J., 2009. Populations of genomic RNAs devoted to the replication or spread of a bipartite plant virus differ in genetic structure. J. Virol. 83 (24), 12973–12983.

Martelli, G.P., Agranovsky, A.A., Bar-Joseph, M., Boscia, D., Candresse, T., Coutts, R.H., Dolja, V.V., Falk, B.W., Gonsalves, D., Jelkmann, W., Karasev, A.V., Minafra, A., Namba, S., Vetten, H.J., Wisler, G.C., Yoshikawa, N., 2002. The family *Closteroviridae* revised. Arch. Virol. 147 (10), 2039–2044.

Mawassi, M., Karasev, A.V., Mietkiewska, E., Gafny, R., Lee, R.F., Dawson, W.O., Bar-Joseph, M., 1995a. Defective RNA molecules associated with *Citrus tristeza virus*. Virology 208 (1), 383–387.

Mawassi, M., Mietkiewska, E., Hilf, M.E., Ashoulin, L., Karasev, A.V., Gafny, R., Lee, R.F., Garnsey, S.M., Dawson, W.O., Bar-Joseph, M., 1995b. Multiple species of defective RNAs in plants infected with *Citrus tristeza virus*. Virology 214 (1), 264–268.

Mawassi, M., Satyanarayana, T., Albiach-Marti, M.R., Gowda, S., Ayllon, M.A., Robertson, C., Dawson, W.O., 2000. The fitness of *Citrus tristeza virus* defective RNAs is affected by the lengths of their 5'- and 3'-termini and by the coding capacity. Virology 275 (1), 42–56.

Ng, J.C.K., Falk, B.W., 2006. *Bemisia tabaci* transmission of specific *Lettuce infectious yellows virus* genotypes derived from *in vitro* synthesized transcript-inoculated protoplasts. Virology 352 (1), 209–215.

Ng, J.C.K., Tian, T., Falk, B.W., 2004. Quantitative parameters determining whitefly (*Bemisia tabaci*) transmission of *Lettuce infectious yellows virus* and an engineered defective RNA. J. Gen. Virol. 85 (9), 2697–2707.

Okuda, M., Okazaki, S., Yamasaki, S., Okuda, S., Sugiyama, M., 2010. Host range and complete genome sequence of *Cucurbit chlorotic yellows virus*, a new member of the genus *Crinivirus*. Phytopathology 100 (6), 560–566.

Rubio, L., Yeh, H.H., Tian, T., Falk, B.W., 2000. A heterogeneous population of defective RNAs is associated with *Lettuce infectious yellows virus*. Virology 271 (1), 205–212.

Salem, N.M., Chen, A.Y.S., Tzanetakis, I.E., Mongkolsiriwattana, C., Ng, J.C.K., 2009. Further complexity of the genus *Crinivirus* revealed by the complete genome sequence of *Lettuce chlorosis virus* (LCV) and the similar temporal expression of LCV genomic RNAs 1 and 2. Virology 390, 45–55.

Sambrook, J., Russell, D.W., 2001. Molecular cloning: a laboratory manual. CSHL Press, Cold Spring Harbor.

Tian, T., Rubio, L., Yeh, H.H., Crawford, B., Falk, B.W., 1999. *Lettuce infectious yellows virus*: *in vitro* acquisition analysis using partially purified virions and the whitefly *Bemisia tabaci*. J. Gen. Virol. 80 (5), 1111–1117.

Tzanetakis, I.E., Susaimuthu, J., Gergerich, R.C., Martin, R.R., 2006. Nucleotide sequence of *Blackberry yellow vein associated virus*, a novel member of the *Closteroviridae*. Virus Res. 116 (1–2), 196–200.

Wang, J., Turina, M., Stewart, L.R., Lindbo, J.A., Falk, B.W., 2009a. Agroinoculation of the *Crinivirus*, *Lettuce infectious yellows virus*, for systemic plant infection. Virology 392 (1), 131–136.

Wang, J., Yeh, H.H., Falk, B.W., 2009b. *cis* preferential replication of *Lettuce infectious yellows virus* (LIYV) RNA 1: the initial step in the asynchronous replication of the LIYV genomic RNAs. Virology 386 (1), 217–223.

Wintermantel, W.M., Wisler, G.C., Anchieta, A.G., Liu, H.Y., Karasev, A.V., Tzanetakis, I.E., 2005. The complete nucleotide sequence and genome organization of *Tomato chlorosis virus*. Arch. Virol. 150 (11), 2287–2298.

Wintermantel, W.M., Hladky, L.L., Gulati-Sakhuja, A., Li, R., Liu, H.Y., Tzanetakis, I.E., 2009. The complete nucleotide sequence and genome organization of *Tomato infectious chlorosis virus*: a distinct crinivirus most closely related to *Lettuce infectious yellows virus*. Arch. Virol. 154 (8), 1335–1341.

Yang, G., Mawassi, M., Ashoulin, L., Gafny, R., Gaba, V., Gal-On, A., Bar-Joseph, M., 1997. A cDNA clone from a defective RNA of *Citrus tristeza virus* is infective in the presence of the helper virus. J. Gen. Virol. 78 (Pt 7), 1765–1769.

Yeh, H.-H., Tian, T., Rubio, L., Crawford, B., Falk, B.W., 2000. Asynchronous accumulation of *Lettuce infectious yellows virus* RNAs 1 and 2 and identification of an RNA 1 trans enhancer of RNA 2 accumulation. J. Virol. 74 (13), 5762–5768.